International Journal on Electrical Engineering and Informatics - Volume 10, Number 1, March 2018

Compressive Sensing Reconstruction Algorithm using L_1-norm Minimization via L_2-norm Minimization

Koredianto Usman[1,3], Hendra Gunawan[2], and Andriyan Bayu Suksmono[1]

[1]School of Electrical and Informatics Engineering, Institut Teknologi Bandung
[2]Faculty of Mathematics and Natural Sciences, Institut Teknologi Bandung
[3]Faculty of Electrical Engineering, Telkom University
Jalan Ganesha No.10, Bandung 40132, Indonesia
Jalan Telekomunikasi No.1 Dayeuhkolot, Jawa Barat, Indonesia
suksmono@stei.itb.ac.id

Abstract: At the moment, there are two main methods of solving the compressive sensing (CS) reconstruction problem which are the convex optimization and the greedy algorithm. Convex optimization has good reconstruction stability but very slow in computation. Greedy algorithm, on the other hand, is very fast but less stable. A fast and stable CS reconstruction algorithm is necessary for a better provision of CS in practical application. In this paper we proposed a CS reconstruction algorithm using L_1-norm minimization via L_2-norm minimization. This method is based on geometrical interpretation of L_1-norm minimization of the reconstruction problem and the fact that the Euclidean distance between L_1-norm and L_2-norm solution lie closely. In other word, if L_2-norm solution is found, then direction to the L_1-norm solution is on the shortest path connecting them. This approach offers a simpler computation. Computer simulation showed that proposed algorithm has better stability than the greedy algorithm and faster computation than the convex optimization. The proposed algorithm thus provides an alternative solution for CS reconstruction problem when a balance between speed and stability is required.

Keywords: compressive sampling, sparse reconstruction, L_1-norm, L_2-norm, convex optimization, greedy algorithm

1. Introduction

In many digital applications, it is common to acquire raw data or raw signal and then compress it using various compression techniques to achieve a smaller data size. The serial processes of acquisition and compression, however, lead to inefficiency since the unnecessary part of signal is acquired and then discarded. The method of compressive sensing or compressive sampling (CS) which works on sparse raw signal is now commonly used to avoid this inefficiency as the acquisition and compression can be processed in single step [1, 2, 3].

In unifying these processes, CS is implemented using either a pre-configurable hardware or software to perform these steps. The result of CS is a compressible form of raw signal with a small size which is efficient for data storing or transmission. As sparse signal occurs in wide area in our daily life, CS has been applied in various applications such as MRI images [4], radar [5], antenna beamforming [6], ground penetrating radar (GPR) [7, 8], image encoding [9], source localization [10], network tomography [11], astronomy imaging [12], and so forth.

In CS, it is often necessary to reconstruct original signal from the compressed signal, for example in MRI image where the original signal need to be recovered to aid the medical examination. The step to recover back the original signal from the compressed signal is called CS reconstruction. At the moment, there are various CS reconstruction algorithms available with two main methods that widely used which are the convex optimization and the greedy algorithm. Convex optimization is based on the mathematical analysis of L_1-norm minimization while greedy algorithm is a heuristic algorithm contains iterative steps, where in each step a local optimum is selected with a hope of a global optimum is obtained at the end of iteration.

Received: February 13rd, 2018. Accepted: March 23rd, 2018
DOI: 10.15676/ijeei.2018.10.1.3

Greedy algorithm has been investigated by many researchers. The result from these researches have produced some important greedy algorithms such as the Matching Pursuit (MP) [13], Orthogonal Matching Pursuit (OMP) [14, 15], regularized OMP (ROMP) [16], Stagewise OMP (StOMP) [17], and Compressive Sampling MP (CoSaMP) [18]. Convex optimization on the other hand, is also investigated by many researchers. Practical software has been developed to solve CS reconstruction problem such as CVX discipline programming (CVX) [19] and L_1-Magic [20].

In general, greedy algorithm offers a faster computation time, but does not always guarantee a correct solution and it suffers in highly correlated environment [21]. On the other hand, convex optimization has better accuracy, but slow in computation [22]. A need for a fast and high accuracy algorithm is apparently important for CS usefulness in many practical applications.

In this paper, we propose a new CS reconstruction algorithm based on minimization of L_1-norm via minimization of L_2-norm. This method offers advantages of faster computation as it exploit the analytical solution of L_2-norm rather than the Newton gradient iteration as in convex optimization. As this method does not take the coherency between the columns in compression matrix as a consideration, this proposed method is also relatively stable in high coherency environment. This algorithm thus combines the advantages of greedy algorithm and convex optimization algorithm.

The presentation of this paper is arranged as follows. Section 2 provides a brief mathematical overview of CS compression, CS reconstruction, the greedy algorithm and convex optimization algorithm. Section 3 describes the detail of the proposed algorithm. Section 4 gives simulation results on the comparison of the proposed algorithm with the greedy algorithm and convex optimization. The capability of the proposed algorithm is also tested using real ground penetrating radar (GPR) signal at the end of Section 4. Section 5 concludes this paper with several outlooks for further research on CS reconstruction. Table 1 shows the list of notations that are used throughout this paper.

Table 1. List of Notations

Notation	The meaning of the notation
$\mathbf{A}^T$	A transpose of matrix **A**
$\mathbf{A}^H$	A transpose conjugate of matrix **A**
$\mathbf{A}^{-1}$	An inverse of matrix **A**
det(**A**)	An operation to calculate determinant of matrix **A**
dim(**A**)	An operation to take the dimension of matrix **A**
$\lvert x \rvert$	An absolute value of a constant x
$\lVert \mathbf{x} \rVert_0$	A zero-order or L_0-norm of vector **x**
$\lVert \mathbf{x} \rVert_1$	A first-order or L_1-norm of vector **x**
$\lVert \mathbf{x} \rVert_2$	A second-order or L_2-norm of vector **x**
$\hat{\mathbf{x}}$	an estimate of vector **x**
$< \mathbf{x} , \mathbf{y} >$	Inner or dot product operation of vector **x** and **y**
argmax(**x**)	An operation to get the index of the maximum value in vector **x**
$\mathbf{A} \cup \mathbf{B}$	Union operation of matrix **A** and matrix **B**

2. Related Work

Before the proposed algorithm is discussed, it is necessary to briefly review the *p*-order norm as a basis of CS reconstruction. It is also necessary to briefly review basic processes in CS compression and reconstruction as these processes provide basis on the proposed method. The greedy algorithm and convex optimization will be discussed in short in this section.

Interested readers can found detail of OMP in the work of Tropp and Gilbert [15], while convex optimization is extensively explained in the work of Boyd and Vandenberghe [22].

A. p-order norm

A norm of a vector provides an important quantity in many mathematical analyses. A *p*-th order norm of a vector $\boldsymbol{x} = [x_1 \quad x_2 \quad \cdots \quad x_N]$ for $p \geq 0$ is defined as

$$\|\mathbf{x}\|_p = \sqrt[p]{x_1^p + x_2^P + \cdots + x_N^P} \tag{1}$$

There are three important values of *p* in CS reconstruction which are 0, 1, and 2. In the case of $p = 0$, which is denoted as zero-order norm (L_0-norm), the norm value represents a number of non-zero elements. In other word, zero-order norm of *x* is equal to the sparsity of the signal. This norm is used as optimization criteria in CS reconstruction. In the case of $p = 1$, the norm is called first-order norm (L_1-norm) which is $\|\mathbf{x}\|_1 = |x_1| + |x_2| + \cdots + |x_N|$. This norm is used as a optimization criteria of a relaxed version of CS reconstruction which is also called as *basis pursuit* (BP). In the case of $p = 2$, the norm is called second-order norm (L_2-norm) which is $\|\mathbf{x}\|_2 = \sqrt[2]{x_1^2 + x_2^2 + \cdots + x_N^2}$. This norm is known geometrically as Euclidean length of vector *x*.

B. CS compression and reconstruction

Generally speaking, CS consists of two steps which are the compression step and reconstruction step. In CS, a discrete signal **x** of length *N* can be compressed into signal **y** of length *M* by multiplying **x** to a matrix **A** which is called sensing matrix or compression matrix with dimension of $M \times N$ ($M < N$),

$$\boldsymbol{y} = \boldsymbol{Ax} \tag{2}$$

The process to produce **y** from **x** using **A** as described in Equation (2) is called CS compression. The step to recover back **x** from **y** and **A** is called the reconstruction step. Although calculating **y** from **A** and **x** is easy, reconstruction **x** from **A** and **y** is difficult as Equation (2) for $M < N$ is an underdetermined system of linear equation with an infinite possible solution. There are two basic CS requirements to obtain a correct solution out of these infinite possible solutions which are: the original signal **x** has to be sparse in certain basis and sensing matrix **A** has to be restricted isometrics property (RIP) compliance.

A signal **b** is called sparse if **b** consists only a few non-zero values where majority of the others are zero. In more general view, a signal b is called sparse in a basis $\boldsymbol{\Psi}$ if

$$\mathbf{b} = \boldsymbol{\Psi}\boldsymbol{\upsilon} \tag{3}$$

for a sparse vector $\boldsymbol{\upsilon}$.

On the other hand, a sensing matrix *A* is called RIP compliance if it fulfills

$$(1-\delta_s)\|\mathbf{x}\|_2 \leq \|\mathbf{Ax}\|_2 \leq (1+\delta_s)\|\mathbf{x}\|_2 \tag{4}$$

for a small positive value δ_s. Equation (4) has a geometrical interpretation that the sensing matrix **A** preserves the Euclidean length of original signal before and after compression. Candes and Tao gave a lengthy mathematical explanation on the role of RIP to the CS reconstruction [23].

After sparsity and RIP requirements are fulfilled, the reconstruction of CS can be solved using minimization L_0-norm which is [1]

$$\hat{x} = \min \|x\|_0 \quad \text{subject to} \quad A \cdot x = y \tag{5}$$

Chen *et al*. however realized that optimization problem in Equation (5) did not lead to any analytical or practical solution [24]. Therefore, they proposed a relaxation from a zero-order norm minimization to a first-order norm minimization, which is

$$\hat{x} = \min \|x\|_1 \quad \text{subject to} \quad A \cdot x = y \tag{6}$$

The formulation in Equation (6) is also called as basis pursuit (BP). Even though Chen et al. did not give a mathematical proof that first-order norm produced similar solution to those of zero-order norm, Donoho in his investigation showed that there is plenty statistical evidence that both solutions are similar [25]. Relaxing L_0-norm to L_1-norm minimization, however, requires higher sparsity in x as indicated by Donoho and Huo [26] and also by Elad and Bruckstein [27].

C. Orthogonal Matching Pursuit

OMP is one of the most important greedy algorithms. While many researchers consider that OMP was derived from MP [13], it was actually developed rather independently by Chen et al. [14] in 1989. The main difference between MP and OMP is on the orthogonalization step which is not available in MP. The introduction of OMP for sparse reconstruction was pioneered by Tropp and Gilbert [15].

For CS reconstruction, greedy algorithm views the sensing matrix **A** as a collection of columns $\mathbf{a_i}$ which is called basis or atom to form a dictionary matrix $\mathbf{A} \in R^{M \times N}$ [13, 14, 15]. Assuming that $x = [x_1 \quad x_2 \quad \cdots \quad x_N]$, the compression process as described in Equation (2) can be viewed as linear combination of a_i by x_i to form **y**, which is

$$\mathbf{y} = x_1\mathbf{a_1} + x_2\mathbf{a_2} + \cdots + x_N\mathbf{a_N} \tag{7}$$

Using this view, OMP algorithm works reversely to find x which is selecting an atom x_i in each step which has the highest contribution to the compressed vector y. After each atom has been selected, OMP calculates the residue vector from compressed vector y and performs the orthogonalization step to ensure that the selected atoms do not alter the calculation of the next atom selection. A complete OMP algorithm is given in the work of Tropp and Gilbert [15].

Algorithm 1 : *Orthogonal Matching Pursuit*
Input : $\mathbf{A} \in \mathbf{R}^{M \times N}$, and $\mathbf{y} \in \mathbf{R}^M$, sparsity level *k*.
Output : $\hat{\mathbf{x}} \in \mathbf{R}^M$.

1: $\mathbf{r}^{(0)} \leftarrow \mathbf{y}$ ▷ *initialize the residual*
2: $\Lambda^{(0)} \leftarrow \{\}$ ▷ *initialize the indices*
3: $\mathbf{A}_{new} \leftarrow \{\}$
4: for $i = 1,\ldots,k$ do
5: $\lambda^{(i)} \leftarrow \arg\max_{j=1,\cdots,n} \left|\left\langle \mathbf{r}^{i-1}, \mathbf{a_j} \right\rangle\right|$ ▷ *the column of A that is most correlated with* $r^{(i-1)}$
6: $\mathbf{\Lambda}^{(i)} \leftarrow \mathbf{\Lambda}^{(i-1)} \cup \boldsymbol{\lambda}_i$
7: $\mathbf{A}_{new}^{(i)} \leftarrow \left[\mathbf{A}_{new}^{(i-1)} \quad \mathbf{a}_{\lambda^{(i)}}\right]$
8: $\mathbf{x}^{(i)} \leftarrow \arg\max_{\hat{\mathbf{x}}} \left\|\mathbf{y} - \mathbf{A}_{new}^{(i)}\hat{\mathbf{x}}\right\|_2$ ▷ *solve the Least Squares for new signal estimate*
9: $\mathbf{a}^{(i)} \leftarrow \mathbf{\Phi}^{(i)}\mathbf{x}^{(i)}$ ▷ *new data approximation*
10: $\mathbf{r}^{(i)} \leftarrow \mathbf{y} - \mathbf{a}^{(i)}$ ▷ *new residual*
11: end for

12: $\hat{\mathbf{x}} \leftarrow \mathbf{x}^{(k)}$
13: *return* $\hat{\mathbf{x}}$

D. Convex Optimization

Convex optimization has become a standard method to solve optimization problem that based on L_1-norm minimization. Solving CS reconstruction problem as stated in Equation (6) using convex optimization is solved by recasting the minimization problem into a Linear Programming (LP). This LP is solved, for example, using the *path following primal-dual method* [19]. Consider the case of CS reconstruction as formulated in Equation (6). We can recast this reconstruction problem into an LP which is [20]

$$\min \sum_i u_i \text{ subject to } x_i - u_i \leq 0 \tag{8}$$

$$-x_i - u_i \leq 0 \tag{9}$$

$$\mathbf{Ax} = \mathbf{y} \tag{10}$$

These set of equations can be solved using a standard primal-dual algorithm with Newton iteration step is given by [20]. In this research, the implementation of CS reconstruction using convex optimization is solved general purpose solver package developed by Stephen Boyd which is called as CVX [20]. This package can be run under engineering computation software such as Matlab or Octave. The following CVX code is an example to solve Equation (6).

```
cvx_begin
      variable x(n)
      minimize norm(x(n),1)
      subject to
            Ax==y
cvx_end
```

3. Proposed Method

The CS reconstruction as given in Equation (6) can be viewed as optimization problem with objective function $f(\mathbf{x}) = \|\mathbf{x}\|_1$ and constraint function $g(\mathbf{x}) = \mathbf{y} - \mathbf{Ax} = 0$. Geometrically, the solution of this optimization problem is to find the touching point between the objective curve and the constraint curve. As an illustration, we consider a simple original signal consist of two samples which is $\mathbf{x} = [x_1 \quad x_2]^T$. The objective function *f*(x) curve forms a four-sided rhombic and the constraint function form a straight line y=Ax as shown in as shown in Figure 1(A). In this figure, the solution of minimization problem is obtained when the rhombic touches the straight line (point P). In the other word, point P is the solution of L_1-norm minimization. The minimization of L_2-norm, on the other hand, can be formulated as

$$\hat{\mathbf{x}} = \min \|\mathbf{x}\|_2 \quad \text{subject to} \quad \mathbf{A} \cdot \mathbf{x} = \mathbf{y} \tag{11}$$

The L_2-norm in this two samples signal forms a circle as shown in Figure 1(A). The solution of L_2-norm minimization is a touching point of the circle and straight line (point Q). Other than point P(0 , x_2), the constraint function $g(x)$ also intersects the coordinate axis at point T (x_1,0). Both point P and point T have the lowest sparsity on the constraint line $g(x)$ which is one. As we observe from Figure 1(A) that the distance from L_2-norm solution (Q) is shorter to the L_1-norm solution (P) than to other point that has the lowest sparsity (T). In the other words, $\|QP\|_2 \leq \|QT\|_2$.

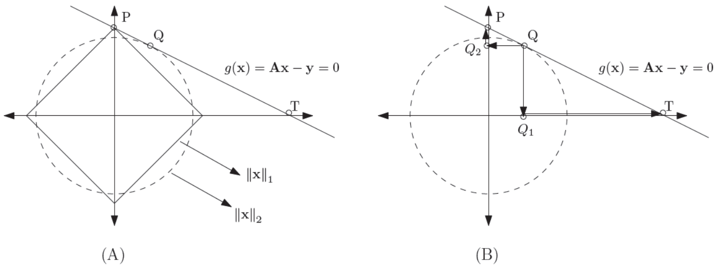

Figure 1. (A) The solution of L_1-norm and L_2-norm minimization that fulfill constraint Ax = y (point P and Q respectively). (B) Projection of point Q to x_1 and x_2 axis.

Based on this observation, we conclude that once the L_2-norm solution has been found, and then the L_1-norm can be found by finding the closest sparse point in constraint line $g(x)$ from L_2-norm solution. The basis of this observation is generalized in Proposition 1.

Proposition 1. *Let P be the L_1-norm point solution of Equation (6) and let Q be the L_2-norm solution of Equation (11). Let also T_i, i = 1, 2, 3, ⋯, s, be intersections of constraint function to the axes of coordinate. The distance from P to Q is the smallest compared to the distance from Q to any other points T_i. That is* $\|QP\|_2 \leq \|QT_i\|_2$ *for all i = 1, 2, ⋯, s.*

The following proposition gives the analytical solution of L_2-norm solution.

Proposition 2. *Let Q be the L_2-norm solution of Equation (11). Then Q can be calculated as: Q = $(AA^T)^{-1}A^T y$.*

The proofs of Proposition 1 and Proposition 2 are given in Appendix.

After L_2-norm has been found, then it is necessary to find the direction from L_2-norm solution (Q) to L_1-norm solution (P). Let us denote the coordinate of point Q as x_Q which is

$$\mathbf{x_Q} = \left(\mathbf{AA}^T\right)^{-1}\mathbf{A}^T\mathbf{y}. \quad (12)$$

To find direction from Q to P, we first project the point Q to x_1 and x_2 axis to obtain points Q_1 and Q_2 respectively (Figure 1(B)). If the coordinate of Q is written in vector as $x_Q=[x_{1Q}, x_{2Q}]^T$, then the point Q_1 and Q_2 have the coordinate as represented by vectors as $[x_{1Q}, 0]^T$ and $[0, x_{2Q}]^T$ respectively. As $\|QP\|_2 \leq \|QT\|_2$ we expect that $\|OQ_1\|_2 \leq \|OQ_2\|_2$, where O denotes the coordinate origin. As $\|OQ_1\|_2 = x_{1Q}$ and $\|OQ_2\|_2 = x_{2Q}$, we conclude that the direction from Q to P is determined by the maximum value of either x_{1Q} or x_{2Q}. In other words, if $x_{1Q} > x_{2Q}$, then the direction from Q to P is by following x_1-axis, while if $x_{1Q} < x_{2Q}$, then the direction from Q to P is by following x_2-axis.

For a general N dimension of signal x and $M \times N$ dimension of matrix **A**, the direction from Q to P can be represented by choosing M largest value in vector L_2-norm solution Q. A direction vector can be now represented as vector **d** with the length of N and has value ones at location corresponding to M largest value in $\mathbf{x_Q}$ while the rest is zeros. Using this direction vector, we can modify the sensing matrix **A** to become $\mathbf{A}_d$ which is

$$\mathbf{A}_d = \mathbf{A} \cdot \mathbf{d} \quad (13)$$

The sensing matrix A_d now contains the correct direction to L_1-norm solution. The L_1-norm solution now can be found as

$$\mathbf{x}_P = \left(\mathbf{A}_d\mathbf{A}_d^{\;T}\right)^{-1}\mathbf{A}_d^T\mathbf{y} \quad (14)$$

where x_p is the coordinate of L_1-norm solution. We now can state our proposed algorithm as follows.

Algorithm 2: *The L_1-norm minimization via L_2-norm minimization*
Input: $y \in \mathbf{R}^M$ and $A \in \mathbf{R}^{M\times N}$, sparsity k
Output: $\hat{\mathbf{x}} \in \mathbf{R}^N$

1:	[M, N] $\leftarrow$ dim(**A**)	▷ *initiate the dimension*
2:	$\gamma \leftarrow \det(\mathbf{A}\mathbf{A}^T)$	
3:	If $\gamma = 0$ then *stop, return* $\hat{\mathbf{x}} \leftarrow \{\}$, else *continue to step 4*	
4:	*calculate* $\boldsymbol{x_Q} \leftarrow (\mathbf{A}\mathbf{A}^T)^{-1}\mathbf{A}^T\mathbf{y}$	▷ *L_2-norm solution*
5:	$[\mathbf{U}\ \ \xi] = \mathrm{sort}(\mathrm{abs}(\boldsymbol{x_Q}))$	▷ *sort L_2-norm solution*
6:	$\mathbf{d_s}$ = *zeros* (*N,1*)	▷ *initiate direction vector*
7:	*for i=1 to k*	
8:	$\mathbf{ds}(\xi\,(k))=1$	▷ *construct vector direction from L_2-norm solution to L_1-norm solution*
9:	*end for*	
10:	$\mathbf{A_s} = \mathbf{Ad_s}$,	
11:	$\mathbf{x_P} = (\mathbf{A_s}\mathbf{A_s}^T)^{-1}\mathbf{A_s}^T\mathbf{y}$	▷ *L_1-norm solution*
12:	$\hat{\mathbf{x}} \leftarrow \mathbf{x_P}$	
13:	return $\hat{\mathbf{x}}$	

In complex valued signals, we use $\mathbf{A}^H$ to denote operation of transpose conjugate of **A** instead of a simple transpose of **A**. In the next section, we will compare the performance of our proposed method with the convex optimization (CVX) and greedy algorithm (OMP).

4. Result and Analysis

To assess the performance of the proposed algorithm, we run computer simulations with various situations such as coherency and noise. We also test the computation speed of the algorithm. As the benchmark, we use CVX programming as the representation of convex optimization, and OMP as the representation of greedy algorithm. The following simulations are performed: reconstruction performance as function of coherency, the performance as function of noise power, the computation time as function of signal length. We also performed the comparison of these algorithms in the case of GPR signal reconstruction. In our experiments, we use root mean square error (RMSE) to measure the closeness between the reconstructed signal $\hat{\mathbf{x}}$ and the original one x. Higher RMSE value means worse performance. RMSE is calculated as

$$RMSE = \sqrt{\frac{1}{N}\sum_{i=1}^{N}\left(x_i - \hat{x}_i\right)^2} \tag{15}$$

A. Performance as function of coherency

This simulation is about the comparison of the performance of proposed method versus OMP and CVX in term of robustness against coherency of the sensing matrix A. Coherency of matrix A is defined as the highest value of inner product of columns in **A**, or mathematically this statement can be written as

$$\gamma(\mathbf{A}) = \max_{j<k}\left(\frac{\left|\left\langle \mathbf{A}(:,j)\cdot\mathbf{A}(:,k)\right\rangle\right|}{\left\|\mathbf{A}(:,j)\right\|_2\left\|\mathbf{A}(:,k)\right\|_2}\right) \tag{16}$$

Coherency value has the value of between $0 \leq \gamma(\cdot) \leq 1$. High value of coherency of **A** indicates that there are at least two columns in **A** that closely correlated. There are some applications when the case of high coherency may take place, for example direction of arrival estimation, when two objects lay closely each other. OMP is well known to be weak in this high coherency environment.

In this simulation, we use two compression ratios which are 2:1 (high compression ratio) and 6:5 (low compression ratio). Compression ratio is defined as the ratio between the lengths of original signal (*N*) to the length of compressed signal (*M*). The values in matrix **A** are randomly generated using Gaussian random distribution (an i.i.d Gaussian distribution). We use a simple method to control the coherency value in **A** which is by modifying column *k* using column *l* *(k* $\neq$ *l)* using linear substitution as follows.

$$\boldsymbol{a_k} \leftarrow \mu \cdot \boldsymbol{a_l} + (1-\mu)\boldsymbol{a_k} \tag{17}$$

We call the parameter μ ($0 \leq \mu \leq 1$) in Equation (17) as coherency control parameter. Increasing the value of μ corresponds to the higher coherency in **A** since *k*-th column becomes more similar to the *l*-th column. We ran the simulation 100 times for each value of μ, and the RMSE is taken as average of the RMSE value of each simulation. The results which corresponds low and high compression ratio are depicted in Figure 2(A) and Figure 2(B) respectively. In these figures, we increase the value of μ gradually from 0.1 to 0.9. The vertical axis corresponds to the RMSE value. In low compression ratio (Figure 2(A)), all methods have a relatively good performance at low value of μ especially below 0.3. As the value of μ increases, the OMP performance decreases rapidly as indicated by high RMSE value. CVX, on the other hand, has a good stable performance as we expect with the RMSE at about 0.14 throughout all the value of μ.

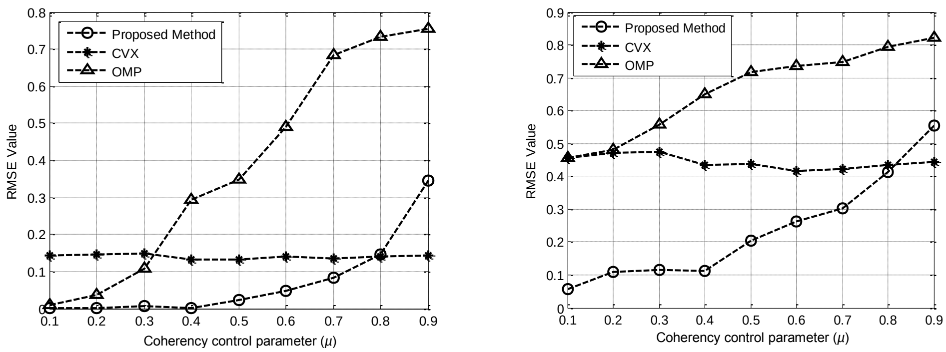

(A) (B)

Figure 2. The RMSE of OMP, CVX and Proposed Method as a function of μ for (a) low compression ratio (6:5) and (b) high compression ratio (2:1).

The proposed method has the best performance at low μ value, and its performance starts to worsen at the value of μ greater than 0.7.

Similar trend is also observed in high compression scheme (Figure 2(B)). However, CVX and OMP scheme have a relatively high RMSE at low value of μ which is about 0.45. The proposed method, in this case, again shows a best performance at μ less than 0.4. At μ greater than 0.4 our proposed method start declining and at μ greater than 0.8, the proposed algorithm performs worse than CVX. CVX maintained a relative constant RMSE value at about 0.45 throughout all values of μ. OMP, on the other hand, has RMSE value which increases as the value of μ increases.

B. Performance as function of SNR

This simulation is aimed to assess how the proposed method performs in noisy environment. To obtain this information, we perform simulations with similar setup to those in Sec. 4.1. Two compression ratios (low and high compression with *M=6 N=12* and *M=10 N=12* respectively) are used as in previous simulation. The elements in matrix **A** are generated randomly using i.i.d. Gaussian distribution. The signal **x** with sparsity of two is generated. After that, the compressed signal **y** is added with additive white Gaussian noise (AWGN) with SNR from 0 to 20 dB with increment of 2 dB. For each simulation, RMSE is calculated and the simulation is repeated 1000 times and averaging the RMSEs.

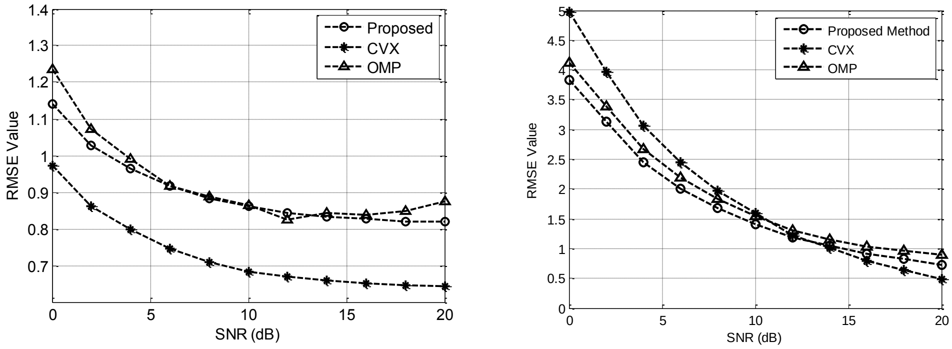

(A) (B)

Figure 3. Performance in noisy environment. (A) low compression ratio

(B) high compression ratio

The average RMSE as function of SNR are plotted in Figure 3(A) and (B). We observe that in both cases that CVX has a better performance, while the proposed method and OMP has about a similar performance. At this low compression scenario, the performance of proposed method is slightly better than OMP in low SNR values, while OMP has slightly better performance in high SNR values (Figure 3(A)). CVX has a clear advantage in low compression ratio as compared to proposed method and OMP. In the case of high compression ratio (Figure 3(B)), the three schemes have about similar performance. Proposed method has best performance at low SNR, with OMP and CVX follow closely. At high SNR values, CVX performs best and followed by proposed method and OMP.

C. The computation time as function of signal length

In Sec. 4.2, we observe that CVX has better performance noisy environment. In this simulation, we will show that the CVX performance has to be paid in a slow reconstruction time. Theoretically, assuming that matrix **A** has dimension of $M \times N$ and signal sparsity k, the complexity of OMP algorithm is $O(kMN)$ [15]. The complexity of convex optimization as reported by Nemirovski is $O(MN^2)$ for calculating Newton's gradient, and $O(N^3)$ to solve the assembled equations. As M << N in the case of CS reconstruction, then complexity in convex optimization is dominated by $O(N^3)$ [28]. From this theoretical view, we expect that the proposed method and OMP will outperform CVX in term of reconstruction time. In this simulation, we performed a computational time simulation as function of the length of original signal **x**. The compression ratio is 2:1 for all simulation. The result is depicted in Figure 4.

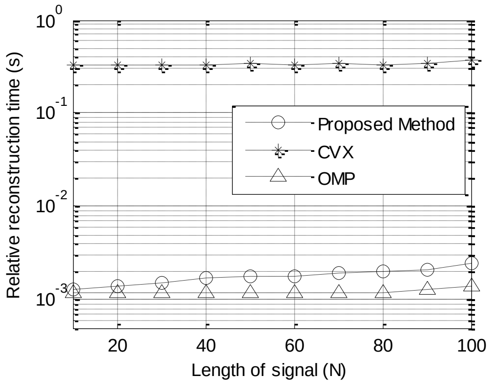

Figure 4. Reconstruction time curve of OMP, CVX, and proposed method as function of signal length.

The relative reconstruction time for each algorithm is relative to the computer being used (Pentium Core 2 Duo 1.6 GHz, 3 GB of RAM). We used Monte Carlo simulation with 1000 repetition in each simulation. The result as shown in Figure 4 clearly indicated that CVX has the slowest computation time. It is more than 200 times slower than those of OMP and the proposed method. OMP itself shows a slightly better speed than the proposed method.

D. The Reconstruction of GPR signal

In this simulation, we compared the reconstruction capability of the three schemes using actual ground penetrating radar (GPR) signal. This signal was obtained from laboratory measurements of an object (a gun) buried at the depth of about 30 cm. GPR imaging was obtained by collecting downward surface scanning at certain discrete positions on the ground surface. These discrete positions are also called the scanning grids. A-scan signal is GPR signal that was obtained at a certain grid point while B-scan GPR signal was obtained using a set of parallel A-scan signals at certain direction. In this simulation, we used A-scan signal which consists of 624 samples. Figure 5(A) shows a time domain of a particular A-scan signal under in this experiment, while Figure 5(B) shows the frequency domain of this signal. From Figure 5(B), we observe that A-scan signal is a sparse signal in frequency domain with the most of its energy lies within one-sixth of its low frequency band. In other word, we expect a compression ratio limit will 6:1 for a good reconstruction result. We apply CS on this A-scan signal using i.i.d. Gaussian random sensing matrix with the compression ratio of 4:1 which is a bit smaller than the limit 6:1. The compression ratio 4:1 is higher than those 6:5 and 2:1 as in Sec. 4.1 and 4.2 to show that the proposed method still have good reconstruction result in this challenging scenario. The reconstruction results for proposed method, CVX and OMP are shown in Figure 6(A), (B), and (C) respectively.

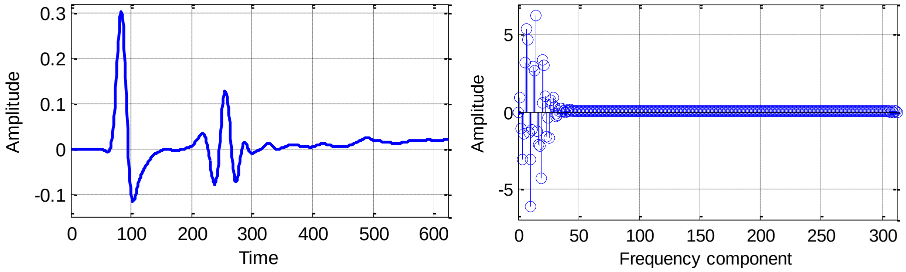

(A) (B)

Figure 5. An example of A-scan from the GPR experiment. (A) in time domain. (B) In frequency domain.

As we observe in Figure 6, the proposed method and OMP has a good reconstruction result where these schemes follow the original signal in entire time frame. CVX, on the other hand, has also a good capability in constructing the trend of the signal but the amplitude estimate is not close to the original signal.

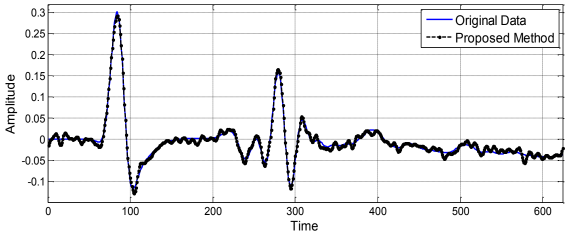

(A)

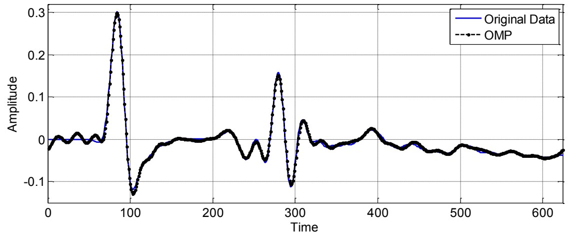

(B)

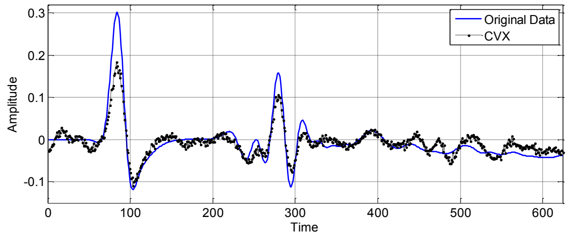

(C)

Figure 6. The reconstruction of GPR A-scan signal. (A) Using proposed method. (B) Using CVX. (C) Using OMP.

5. Conclusion

In this paper we propose a new CS reconstruction algorithm based on L_1-norm minimization via L_2-norm minimization. This algorithm is based on geometrical interpretation of L_2-norm solution is closed to the L_1-norm solution. The proposed method basically consists of three steps which are: calculating the L_2-norm solution, finding the direction from L_2-norm solution to L_1-norm solution, and calculating L_1-norm solution. The proposed method has a faster computation time as compared to CVX method which is based on heavy Newton iteration. Computer simulation result showed that computation time of the proposed method is more than 200 times faster than those of CVX. The proposed method also does not work on column based, thus it is more robust to the sensing matrix coherency as compared to OMP algorithm. Given these advantages of proposed methods, in term of robustness against noisy, CVX still performs better than the proposed method as Newton iteration is more robust in noisy environment. The proposed method is also slightly slower than OMP due to the sorting step in proposed method which is not available in OMP. In the future, it is still necessary to improve the proposed method so that its speed can be even better.

6. References

[1]. Donoho, D.L., ”Compressed sensing”, *IEEE Transactions on Information Theory*, 52(4), 1289-1306, 2006.

[2]. Candes, E., and Wakin, M.B., ”Compressive sampling”, *Proceedings of the International Congress of Mathematicians*, Madrid, Spain, 25(2), 21- 30, *2008*.

[3]. Baraniuk, R., ”Compressive sensing”. *IEEE Signal Processing Magazine*, 24(4), 118-121, 2007.

[4]. Lustig, M., Donoho, D., Santos, J., and Pauly, J., ”Compressed sensing MRI”, *IEEE Signal Processing Magazine*, 25(2), 72-82, 2008.

[5]. Suksmono, A. B., ”Improved Compressive Sampling SFCW Radar by Equipartition of Energy Sampling”, IJEEI, Vol. 6, No. 3, 2014.

[6]. Edelmann, G. F. and Gaumond, C. F., ”Beamforming using compressive sensing”, *J. Acoust. Soc. America*, 130(4), 2011.

[7]. Gurbuz, A. C., McClellan, J. H., and Scott, W. R., ”A compressive sensing data acquisition and imaging method for stepped frequency GPRs”. *IEEE Transactions on Signal Processing*, 57(7), 2640-2650, 2009.

[8]. Suksmono, A. B., Bharata, E., Lestari, A. A., Yarovoy, A. G., and Ligthart, L. P., ”Compressive stepped-frequency continuous-wave ground penetrating radar”. *IEEE geoscience and remote sensing letters*, 7(4), 665-669, 2010.

[9]. Wahidah, I., Suksmono, A., and Mengko, T., ”A comparative study on video coding techniques with compressive sensing”, *International Conference on Electrical Engineering and Informatics* (ICEEI), pp. 1–5, 2011.

[10]. Malioutov, D., Cetin, M., and Willsky, A., ”A sparse signal reconstruction perspective for source localization with sensor arrays”, *IEEE Transactions on Signal Processing*, 2005, *53*, 3010-3022, 2005.

[11]. Firooz, M. H. and Roy S., ”Network Tomography via Compressed Sensing”, *Proc. IEEE Globecom*, pp.1-5. Dec 2010.

[12]. Suksmono, A. B., ”Interpolation of PSF based on compressive sampling and its application in weak lensing survey”, *Monthly Notices of the Royal Astronomical Society*, 443(1), 919-926, 2014.

[13]. Mallat, S. and Zhang, Z., ”Matching pursuits with time - frequency dictionaries”. *IEEE Transactions on Signal Processing*, 41(12), 3397-3415, 1993.

[14]. Chen, S., Billings, S. A., and Luo, W., ”Orthogonal least squares methods and their application to non-linear system identification”. *International Journal on Control*, 50(5), 1873-1896, 1989.

[15]. Tropp, J. A. and Gilbert, A.C., ”Signal recovery from random measurements via orthogonal matching pursuit”, *IEEE Transactions on Information Theory*, 53(12), 4655-4666., 2007

[16]. Needell, D. and Vershynin, R., ”Signal recovery from incomplete and inaccurate measurements via regularized orthogonal matching pursuit”. *IEEE Journal of Selected Topics in Signal Processing*, 4(2), 310-316, 2010.

[17]. Donoho, D.L., Tsaig, Y., Drori, I. and Starck, J.L., ”Sparse solution of underdetermined systems of linear equations by stagewise orthogonal matching pursuit”. *IEEE Transactions on Information Theory*, 58(2), 1094-1121, 2012.

[18]. Needell, D. and Tropp, J. A., ”Cosamp: Iterative signal recovery from incomplete and inaccurate samples”. *Appl. Comput. Harmon. Anal.*, 26, 301-321, 2008.

[19]. Boyd, S., ”CVX: Matlab software for disciplined convex programming”, Retrieved October 10, 2016, from http://cvxr.com/cvx/, 2014.

[20]. Candes, E. and Romberg, J., ”L1-magic : Recovery of sparse signals via convex programming”. Retrieved October 10, 2016, from http://users.ece.gatech.edu/~justin/l1magic/

[21]. Schnass, K. and Vandergheynst, P., ”Dictionary preconditioning for greedy algorithms”, *IEEE Transactions on Signal Processing*, 56(5), 2008.
[22]. Boyd, S. and Vandenberghe, L., ”Convex optimization”. *Cambridge University Press*, 2004.
[23]. Candes, E. and Tao, T., ”Decoding by Linear Programming”, *IEEE Transactions on Information Theory*, 51, 4203-4215, 2005.
[24]. Chen, S. S., Donoho, D. L. and Saunders, M. A., ”Atomic Decomposition by Basis Pursuit”, *SIAM Review, Society for Industrial and Applied Mathematics*, 43, 129-159, 2001.
[25]. Dohono, D. L., ”For most large underdetermined systems of linear equations the minimal L1-norm solution is also the sparsest solution”, *Comm. Pure Appl. Math*., 59(6), 797-829., 2006.
[26]. Donoho, D. L. and Huo, X., ”Uncertainty principles and ideal atomic decomposition”, *IEEE Transactions on Information Theory*, 47(7), 2845-2862, 2001.
[27]. Elad, M. and Bruckstein, A. M., ”A generalized uncertainty principle and sparse representation in pairs of bases”. *IEEE Transactions on Information Theory*, 48(9), 2558-2567, 2002.
[28]. Nemirovski, A., ”Lecture Notes : Interior Point Polynomial Time Methods In Convex Programming*”, School of Industrial and Systems Engineering*, Georgia Institute of Technology,2004

Appendix

Proof of Proposition 1. For this proof, we use Figure 1(B) as reference. Let the $T_1, T_2, \ldots T_S$ be any other intersections of the constraint curve to the axis of coordinate and let O be the center of the coordinate. Since P is the L_1-norm solution of Equation (6), then $\|OP\|_2 < \|OT_i\|_2$ *for all i = 1, 2, ..., S.* The sign < is strictly without equal sign (=) since the L_1-norm solution is unique. We also note that, since P and Q lie on Ax = y, and since point Q is the point on Ax = y that has the shortest distance from O, it is also true that $\|OQ\|_2 < \|OP\|_2$. From these results we conclude that $\|OQ\|_2 \le \|OP\|_2 < \|OT_i\|_2$ *for all i = 1, 2,…, S.* Now $\|QP\|_2 = \sqrt{\|OP\|_2^2 - \|OQ\|_2^2}$ and $\|QT_i\|_2 = \sqrt{\|OT_i\|_2^2 - \|OQ\|_2^2}$. As $\|OP\|_2 < \|OT_i\|_2$, we conclude that $\|QP\|_2 < \|QT_i\|_2$.

Proof of Proposition 2. We combine the objective and constraint function from Equation (11) using Lagrange multiplier, which is

$$f(\mathbf{x},\boldsymbol{\lambda}) = \|\mathbf{x}\|_2^2 + \boldsymbol{\lambda}^T(\mathbf{y}-\mathbf{Ax}) = \mathbf{x}^T\mathbf{x} + \boldsymbol{\lambda}^T(\mathbf{y}-\mathbf{Ax}) \tag{A.1}$$

Differentiate $f(\mathbf{x},\boldsymbol{\lambda})$) with respect to x and set it equal to 0, we obtain

$$\frac{\partial f(\mathbf{x},\boldsymbol{\lambda})}{\partial \mathbf{x}} = 2\mathbf{x} - \boldsymbol{\lambda}^T\mathbf{A} = 2\mathbf{x} - \mathbf{A}^T\boldsymbol{\lambda} = 0 \tag{A.2}$$

Pre-multiply (A.2) with A and remembering that Ax = y, we obtain

$$2\mathbf{Ax} - \mathbf{AA}^T\boldsymbol{\lambda} = 2\mathbf{y} - \mathbf{AA}^T\boldsymbol{\lambda} = 0 \tag{A.3}$$

Solving for $\boldsymbol{\lambda}$, we obtain

$$\boldsymbol{\lambda} = (\mathbf{AA}^T)^{-1}2\mathbf{y} \tag{A.4}$$

Finally, we substitute (A.4) to (A.2), and solve it for x, we get

$$\mathbf{x} = \mathbf{A}^T(\mathbf{AA}^T)^{-1}\mathbf{y} \tag{A.5}$$

Koredianto Usman is a doctoral student at School of Electrical and Informatics Engineering, Institut Teknologi Bandung (Indonesia). He obtained Bachelor Degree in Electrical Engineering from Institut Teknologi Bandung in 1999 and Master Degree in Telecommunication Engineering Technical University of Munich, Germany in 2001. His researches interests are in fields of signal processing, signal reconstruction, compressive sensing, and radar. He works as lecturer at Faculty of Electrical Engineering, Telkom University (Indonesia).

Hendra Gunawan obtained his bachelor degree from Department of Mathematics, Bandung Institute of Technology. His Ph.D. degree was earned from School of Mathematics, the University of New South Wales in 1992. Prof. Gunawan is currently a professor of mathematics at Bandung Institute of Technology. He belongs to the Analysis and Geometry Group at Faculty of Mathematics and Natural Sciences. His areas of interest are Fourier analysis, functional analysis, and their applications. In 2009, he received an Australian Alumni Award for Excellence in Education, presented by Australia Education International in Jakarta. In 2015, he was elected as a member of the Indonesian Academy of Science (AIPI). In 2016, Prof. Gunawan received a Habibie Award for Basic Sciences.

Andriyan Bayu Suksmono obtained his BS in Physics and MS in Electrical Engineering from Institut Teknologi Bandung (ITB), Indonesia, in 1990 and 1996, respectively. He completed his PhD in 2002 from The University of Tokyo, Japan. He joined the Department of Electrical Engineering of ITB in 1996 as an Instructor. In 2009, he was appointed as a Professor of the School of Electrical Engineering and Informatics, ITB. Prof. Suksmono is a senior member of IEEE. His main research interests are signal processing and imaging.